

Overall Structure Calibration of 3-UCR Parallel Manipulator Based on Quaternion Method

Gang Cheng* – Wei Gu – Jing-li Yu – Ping Tang

China University of Mining and Technology, College of Mechanical and Electrical Engineering, China

In this article a simple yet effective approach for the structure calibration of a three degree-of-freedom (DOF) parallel manipulator is presented. In this approach, the model of the pose error expressed by the Quaternions Parameters was established, based on complete differential-coefficient theory. This was followed by an investigation into the degree of influences represented as sensitivity percentages, of source errors on the pose accuracy with the aid of a statistical model of sensitivity coefficients. Then, the kinematic calibration model with the successive approximation algorithm was achieved. The simulation has been carried out to verify the effectiveness of the proposed algorithm and the results show that the accuracy of the calibration can be significantly improved.

©2011 Journal of Mechanical Engineering. All rights reserved.

Keywords: 3-UCR parallel manipulator, complete differential-coefficient theory, Quaternion, least squares method, sensitivity model, kinematic calibration

0 INTRODUCTION

Parallel manipulators have particularly aroused interest of researchers over the past several decades for their properties of better structural rigidity, positioning accuracy, and dynamic performances [1] and [2]. Unlike serial manipulators, which suffer from the accumulation of joint errors, parallel manipulators are considered to have high accuracy [3]. However, relative investigations have shown that the parallel manipulator is not necessarily more accurate than a serial manipulator with the same manufacturing and assembling precision [4]. Accuracy remains a bottleneck for further industrial applications of parallel manipulators. Therefore, in order to enhance the precisions of parallel manipulators, it is important to evaluate the end-effector's accuracy in the design phase, and to calibrate the kinematic parameters after manufacturing [3]. From kinematic characteristics of lower-mobility parallel manipulators, it can be seen that complete errors compensation of the pose can not be achieved since it does not have six components in terms of both translation and orientation [5]. Therefore, the calibration method effectively reducing the pose errors of end effector is important.

Sensitivity analysis and error identification are necessary for the purpose of better kinematic

characteristics of parallel manipulators. The kinematic parameters with higher sensitivity should be found and controlled strictly. Aiming at optimizing a class of 3-DOF parallel manipulators with parallelogram struts, Huang established a statistical sensitivity model and showed quantitatively the effect of geometrical errors on the pose of end effectors [5]. Based on the sensitivity analysis, Alici optimized the dynamic equilibrium of a planar parallel manipulator [6]. Pott gave the sensitivity model by a simplified force-based method and validated the algorithm by examples of both serial and fully parallel manipulators [7]. In order to study the relations between sensitivity and geometric parameters, Binaud compared the sensitivity of five planar parallel manipulators of different architectures [8]. Therefore, estimating sensitivity of kinematic parameters and studying the priority of kinematic parameters with higher sensitivity can effectively improve the calibration of manipulators.

In the course of structure calibration, for formulating universal functions of errors between the measured and theoretical values, it is feasible to realize the static error compensation of a parallel manipulator by modifying the kinematic parameters based on the calibration model. According to the measuring instruments, calibration methods can be classified into three categories: constrained calibration method, auto-

*Corr. Author's Address: College of Mechanical and Electrical Engineering,
China University of Mining and Technology, 221008, Xuzhou, China, chg@cumt.edu.cn

calibration or self-calibration method, external calibration method [9]. External calibration methods are based on measurements of the end-effector poses through an external device such as laser systems [10], theodolite [11], coordinate measuring machine [12] or camera systems [13]. Constrained calibration methods impose mechanical constraints on the manipulators during the calibration process through a locking device [14]. Auto-calibration or self-calibration methods rely on the measurements of the internal sensors of the manipulators. These methods have two possible approaches: the self-calibration method with redundant information [16] and [17] and the self-calibration method without redundant information [17] and [18]. Although the calibration of parallel manipulators had been study extensively and many novel methods of calibration had been presented, these studies merely focused on all kinematic parameters without sensitivity analysis. In practice, due to the impossible compensation fully of lower-mobility parallel manipulator, it is critical to judge the priority of the kinematic parameters of these manipulators by their sensitivity coefficients.

This article is organized in the following manner. In Section 1, the prototype of the parallel manipulator is described, and its corresponding error model is established based on the complete differential-coefficient matrix theory. Thereafter, the statistical model of sensitivity is studied by normalizing all error sources in the reachable workspace. In Section 2, considering the sensitivity of kinematic parameters, the calibration model and the corresponding algorithm is presented. In Section 3, the numerical simulations of sensitivity and calibration were analyzed respectively, and in the last section the paper is concluded with a number of conclusions.

0.1 Nomenclature

a_i the fix points of the joints in the moving platform
 A_i the fix points of the joints in the base
 B the base

$D_{O'}, D_E$ the orientation matrix of the moving platform and the calibrated point on the end effector
 D_{O3} the third row of the orientation matrix of the moving platform
 E_W, E_{WS} the orientation matrix consisting of the theoretical values and the measured values respectively
 E_{xyz} the geometrical vector of the calibrated point
 Δe_{Eij} the j^{th} offset that need to be calibrated
 δE_R the error matrix of kinematic parameters
 δE_{Ri} the i^{th} error source in δE_R
 ΔE_{Si} the error matrix of the end effector
 ΔE_S the corresponding norm of the pose errors of the end effector
 J_R the Jacobi matrix of calibration
 J_{Ri} the Jacobi submatrix of calibration
 L_B the length of the equilateral triangle lines in the base
 $r_i (i=1,2,3)$ the lengths of the limbs are given as r_i
 L_m the length of the equilateral triangle lines in the moving platform
 L_{OE} the length of the end effector which is perpendicular to the moving platform
 m the moving platform
 $O - XYZ$ the absolute coordinate system attached to the base
 $O' - X'Y'Z'$ the relative coordinate system attached to the moving platform
 T_R the mapping between the pose errors of the end effector and the pose errors of the inputs
 T_{R6i} the sixth row and the i -th column in T_R
 V the volume of workspace
 x_E, y_E, z_E the coordinates of the point E on the end effector
 E The end point of the end effector on the moving platform
 $\hat{p}_i (i=1,2,3)$ the components of principal vector of rotation p referred to the body axes

q_0, q_1, q_2, q_3	the Unit Quaternion parameters
X'_q, Y'_q, Z'_q	the quaternion representation of axes (X', Y', Z') of m
X_q, Y_q, Z_q	the quaternion representation of axes (X, Y, Z) of B
η	the ratio of the fix radiuses of the base and the moving platform
$\overline{OA_i}, \overline{A_i a_i}, \overline{O'a_i}, \overline{OO'}$	the vector $OA_i, A_i a_i, O'a_i$ and OO' , respectively
$\overline{\tau_{Ri}}$	the sensitivity coefficients of error sources

1 SENSITIVITY MODEL

1.1 Quaternion Parameters

In October 1843, William Rowan Hamilton formulated quaternions [18]. The quaternion parameters have several advantages over other orientation parameters as an attitude representation [19]. Quaternion is an appropriate tool for transformation of multiple orientations and control algorithms. The attitude representation based on direction-cosine matrix needs 9 parameters, and Euler angles needs 3 parameters. Compared to direction-cosine matrix, quaternion needs only 4 parameters and only has one constrained equation, while direction-cosine matrix has six constrained equations. Compared to Euler angles, quaternion does not degenerate at any point and avoids the problem of calculation singularity [18].

Quaternion can be represented as the sum of a scalar and a vector [18] and [19], composed by Rodrigues-Hamilton parameters $(q_0, q_i, i = 1, 2, 3)$. By introducing abstract symbols k_1, k_2, k_3 which are the imaginary unit of complex numbers and satisfying the rules $k_{12} = k_{22} = k_{32} = k_1 k_2 k_3 = -1$, the analytical expression for Quaternion q is derived as below:

$$q = q_0 + q_1 k_1 + q_2 k_2 + q_3 k_3, \quad (1a)$$

where 4 components $q_0, q_i, (i = 1, 2, 3)$ satisfy the constraint $q_0^2 + q_1^2 + q_2^2 + q_3^2 = 1$.

The relative coordinate system $O-X'Y'Z'$ on the moving platform m can coincide with the absolute coordinate system $O-XYZ$ by a rotation about the unit u $(\cos\alpha_1 \cos\alpha_2 \cos\alpha_3)^T$ axis through an angle $2\theta_u$ [20]. Quaternion q (q_0, q_1, q_2, q_3) corresponding to the transformation is defined by

the angle θ_u and the unit axis u . The orientation of m can be defined completely by the Euler parameters θ_u and α_i , and it can also be defined completely by the Quaternion q (q_0, q_1, q_2, q_3) . The relationship between Euler parameters (θ_u, α_i) and Rodrigues-Hamilton parameters can be expressed as follows:

$$q_0 = \cos\theta_u, q_1 = \sin\theta_u \cdot \cos\alpha_i, (i=1, 2, 3). \quad (1b)$$

If the Quaternion $X'_q = (0, X')$, $Y'_q = (0, Y')$, $Z'_q = (0, Z')$, $X_q = (0, X)$, $Y_q = (0, Y)$ and $Z_q = (0, Z)$, is associated respectively, with three-dimensional vectors (X', Y', Z', X, Y, Z) and define the operation with the unit Quaternion q , as:

$$X = q \circ X' \circ q^{-1}, Y = q \circ Y' \circ q^{-1}, Z = q \circ Z' \circ q^{-1} \quad (2)$$

where “ \circ ” means Quaternion multiplication, and q^{-1} is the inverse Quaternion of q . Both of them satisfy $q^{-1}q = 1$. Then this transformation, from X'_q to X_q , from Y'_q to Y_q , and from Z'_q to Z_q , represents a rotation from $O-X'Y'Z'$ to $O-XYZ$.

Therefore, the direction-cosine matrix based on Quaternion parameters [21] can be written as:

$$D_{O'} = \begin{bmatrix} 2q_0^2 + 2q_1^2 - 1 & 2(q_1 q_2 - q_0 q_3) & 2(q_1 q_3 + q_0 q_2) \\ 2(q_1 q_2 + q_0 q_3) & 2q_0^2 + 2q_2^2 - 1 & 2(q_2 q_3 - q_0 q_1) \\ 2(q_1 q_3 - q_0 q_2) & 2(q_0 q_1 + q_2 q_3) & 2q_0^2 + 2q_3^2 - 1 \end{bmatrix}. \quad (3)$$

1.2 System Description

The symmetrical parallel manipulator consist of a fixed base, a moving platform and three identical limbs, and its topological structure is described in Fig. 1. $O-XYZ$ is the absolute coordinate system attached to the fixed base, while $O-X'Y'Z'$ is the relative coordinate system attached to the moving platform. The equilateral triangle lines of the moving platform and the fixed base are denoted as $L_{ai aj}$ and $L_{Ai Aj}$ $(i, j = 1, 2, 3; i \neq j)$, respectively, while their corresponding length is denoted as L_m and L_B , respectively. Each limb connects the moving platform to the base by a universal joint (U) at a_i , followed by a cylindrical joint (C) and a revolute joint (R) at A_i , where the cylindrical joint is driven by a ball screw linear actuator. The installation form of these joints provides the manipulator with 3 DOF, one translational motion along the Z-axis and two rotational motion about X-axis and

Y-axis, respectively. The r_i ($i=1, 2, 3$) stands for the lengths of the three limbs. The end effector is assumed to be perpendicular to the moving platform at point O' , and its length is denoted as $L_{O'E}$.

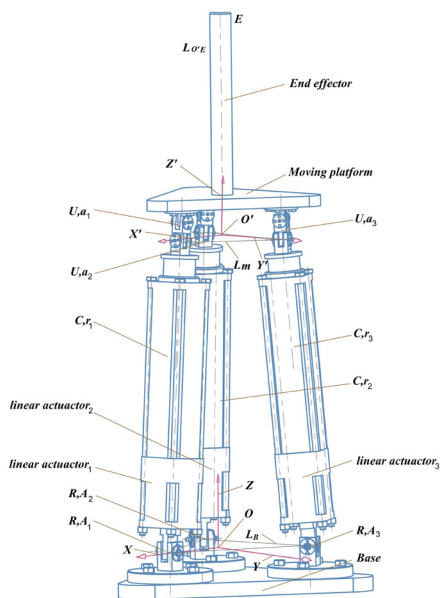


Fig. 1. Symmetrical parallel bionic robot leg with three UCR limbs

1.3 Error Model

$OA_i a_i O'O$ and $OO'E O$ in the 3-UCR parallel manipulator are considered as the closed-loop kinematic chains, and the following equation can express the spatial vector of the drive limbs.

$$\overline{A_i a_i} = \overline{OE} + \mathbf{D}_{O'} \overline{O' a_{iO'}} - \mathbf{D}_{O_3} L_{O'E} - \overline{OA_i}, \quad (4)$$

where the vectors of $\overline{O' a_{iO'}}$ and $\overline{O'E O'}$ with reference to the relative coordinate system can be denoted as $\overline{O' a_i}$ and $\overline{O'E O'}$, respectively. The orientation matrix of the moving platform can be denoted as $\mathbf{D}_{O'}$ and \mathbf{D}_{O_3} denotes the third row of it. The vector of $\overline{O'E}$ can be described by $[0 \ 0 \ L_{O'E}]^T$ by analyzing its spatial relation.

In the process of error transmission, the nominal numbers are different to the effective displacements of the structure parts. By complete differential calculation to the outputs of the parallel manipulator, the error effects can be fully studied, and Eq. (4) can be expressed as follows:

$$r_i \delta \overline{e_{r_i}} + \delta r_i \overline{e_{r_i}} - \delta \overline{OE} - \overline{O' a_{iO'}} \delta \mathbf{D}_{O'} - \mathbf{D}_{O'} \delta \overline{O' a_{iO'}} + L_{O'E} \delta \mathbf{D}_{O_3} + \mathbf{D}_{O_3} \delta L_{O'E} + \delta \overline{OA_i} = 0. \quad (5)$$

Due to $\overline{e_{r_i}}^T \overline{e_{r_i}} = 1$ and $\overline{e_{r_i}}^T \delta \overline{e_{r_i}} = 0$, left-multiplied by $\overline{e_{r_i}}^T$, the Eq. (5) can be simplified as Eq. (6), where δr_i and $\delta \overline{OE}$ equal to $[\delta r_1 \ \delta r_2 \ \delta r_3]$ and $[\delta x_E \ \delta y_E \ \delta z_E]^T$, respectively. $\overline{e_{r_i}}^T \mathbf{D}_{O'}$ and $\mathbf{D}_{O'} \overline{O' a_{iO'}}$ equal to $[T_{D11} \ T_{D12} \ T_{D13}]$ and $[T_{I1} \ T_{I2} \ T_{I3}]^T$, respectively, where $\overline{e_{r_i}}$ denotes the corresponding unified vector of the drive limbs:

$$\delta r_i - \overline{e_{r_i}}^T \delta \overline{OE} - \overline{e_{r_i}}^T \delta \mathbf{D}_{O'} \overline{O' a_{iO'}} - \overline{e_{r_i}}^T \mathbf{D}_{O'} \delta \overline{O' a_{iO'}} + \overline{e_{r_i}}^T L_{O'E} \delta \mathbf{D}_{O_3} + \overline{e_{r_i}}^T \mathbf{D}_{O_3} \delta L_{O'E} + \overline{e_{r_i}}^T \delta \overline{OA_i} = 0. \quad (6)$$

$$T_{i1} \delta x_E + T_{i1} \delta x_E + T_{i1} \delta x_E + T_{i1} \delta x_E + T_{i1} \delta x_E + T_{i1} \delta x_E = 0, \quad i = 1, 2, 3. \quad (7)$$

Substituting the above expressions into Eq. (6), the equation can be rearranged.

In order to solve the six output parameters, a system of six equations should be founded. From Eq. (7), other three simultaneous equations are required. According to the kinematic model based on Quaternions parameters of the parallel manipulator conducted in previous section, three corresponding equations are obtained as follows:

$$x_E = -\frac{2L_m}{\sqrt{3}} q_1 q_2 + 2q_0 q_2 L_{O'E}, \quad (8)$$

$$y_E = \frac{L_m}{2\sqrt{3}} (-1 - 2q_1^2 + 4q_2^2) - 2q_0 q_1 L_{O'E}, \quad (9)$$

$$q_3 = 0, \quad (10)$$

where x_E and y_E denote the coordinates of the point E on the end effector.

By substituting $q_0 = \sqrt{q_1^2 + q_2^2 + q_3^2}$ into Eqs. (8), (9) and (10), the corresponding complete differential forms of the three equations can be rearranged as follows:

$$T_{i1} \delta x_E + T_{i2} \delta y_E + T_{i3} \delta z_E + T_{i4} \delta q_1 + T_{i5} \delta q_2 + T_{i6} \delta q_3 = 0, \quad i = 4, 5, 6. \quad (11)$$

Eqs. (7) and (11) can be rearranged in matrix form:

$$\begin{bmatrix} T_{11} & T_{12} & T_{13} & T_{14} & T_{15} & T_{16} \\ T_{21} & T_{22} & T_{23} & T_{24} & T_{25} & T_{26} \\ T_{31} & T_{32} & T_{33} & T_{34} & T_{35} & T_{36} \\ T_{41} & T_{42} & T_{43} & T_{44} & T_{45} & T_{46} \\ T_{51} & T_{52} & T_{53} & T_{54} & T_{55} & T_{56} \\ T_{61} & T_{62} & T_{63} & T_{64} & T_{65} & T_{66} \end{bmatrix} \begin{bmatrix} \delta x_E \\ \delta y_E \\ \delta z_E \\ \delta q_1 \\ \delta q_2 \\ \delta q_3 \end{bmatrix} = \begin{bmatrix} T_{17} \\ T_{27} \\ T_{37} \\ T_{47} \\ T_{57} \\ T_{67} \end{bmatrix} = \mathbf{T}_{2} \delta \mathbf{E}_R, \quad (12)$$

where $\delta \mathbf{E}_R$ denotes the error matrix of kinematic parameters, and can be expressed as follows:

$$\delta \mathbf{E}_R = [\delta L_{O'E}, \delta L_m, \delta r_1, \delta L_{O'a_x}, \delta L_{O'a_y}, \delta L_{O'a_z}, \delta L_{O'A_x}, \delta L_{O'A_y}, \delta L_{O'A_z}, \delta r_2, \delta L_{O'a_x}, \delta L_{O'a_y}, \delta L_{O'a_z}, \delta L_{O'A_x}, \delta L_{O'A_y}, \delta L_{O'A_z}, \delta r_3, \delta L_{O'a_x}, \delta L_{O'a_y}, \delta L_{O'a_z}, \delta L_{O'A_x}, \delta L_{O'A_y}, \delta L_{O'A_z}]^T, \quad (13)$$

where $\delta L_{O'E}$ and δL_m denote the length error of the end effector and the triangle line error on the moving platform, respectively. δr_i represents the length errors of the drive limbs. $\delta L_{O'a_x}$, $\delta L_{O'a_y}$ and $\delta L_{O'a_z}$ denote the coordinate errors of the connectors on the m . Note that these errors are referenced to the absolute coordinate system. Similarly, the coordinate errors of the connectors on the B are represented by $\delta L_{O'A_x}$, $\delta L_{O'A_y}$ and $\delta L_{O'A_z}$.

The error model of the parallel manipulator describing the relations between errors of kinematic parameters and output parameters can be obtained by the above equations.

1.4 Sensitivity Model

Through the establishment of the probability model of the parallel manipulator, the effects on the pose of the end effector caused by the geometrical errors of manufacture and assembly can be studied statistically. According to the error model of the manipulator, Eq. (12) is rewritten as:

$$\delta \mathbf{E}_S = \mathbf{T}_R \delta \mathbf{E}_R, \quad (14)$$

where \mathbf{T}_R representing the mapping between the pose errors of the end effector and the pose errors of the inputs which denoted as $\delta \mathbf{E}_S$ equals to $\mathbf{T}^{-1} \mathbf{T}_2$.

In order to characterize the standard deviations of the pose errors of the end effector caused by the unified standard deviations of error

sources in the parallel manipulator, it should be assumed that all elements in $\delta \mathbf{E}_R$ are independent statistically and the mean of the elements equals zero. According to the error transmission matrix, the mathematical expectation of $\delta \mathbf{E}_S$ is zero. Therefore, the corresponding variance of $\delta \mathbf{E}_S$ can be derived as follows:

$$D(\delta \mathbf{E}_S) = E(\delta \mathbf{E}_S^2). \quad (15)$$

Rearranging the Eq. (14) gives:

$$\delta \mathbf{E}_S^2 = \delta \mathbf{E}_R^T \mathbf{T}_R^T \mathbf{T}_R \delta \mathbf{E}_R = \left[\sum_{i=1}^{23} \delta E_{Ri} T_{R1i} \cdots \sum_{i=1}^{23} \delta E_{Ri} T_{R6i} \right]_{1 \times 6} \begin{bmatrix} \sum_{i=1}^{23} T_{R1i} \delta E_{Ri} \\ \vdots \\ \sum_{i=1}^{23} T_{R6i} \delta E_{Ri} \end{bmatrix}_{6 \times 1}, \quad (16)$$

where the i^{th} error source in $\delta \mathbf{E}_R$ is denoted as δE_{Ri} , the element in the sixth row and i^{th} column of \mathbf{T}_R is denoted as T_{R6i} . Assuming that the elements in $\delta \mathbf{E}_R$ are independent statistically, we get:

$$\delta \mathbf{E}_S^2 = \sum_{i=1}^{23} \sum_{j=1}^6 T_{Rji}^2 \delta E_{Ri}^2. \quad (17)$$

Substituting Eq. (17) into Eq. (15), the following equation is derived:

$$D(\delta \mathbf{E}_S) = \sum_{i=1}^{23} \sum_{j=1}^6 T_{Rji}^2 E(\delta E_{Ri}^2). \quad (18)$$

Therefore, relations between standard deviations of $\delta \mathbf{E}_R$ and $\delta \mathbf{E}_S$ can be formulated as follows:

$$\sigma(\delta \mathbf{E}_S) = \sqrt{\sum_{i=1}^{23} \sum_{j=1}^6 T_{Rji}^2 \sigma(\delta E_{Ri}^2)}. \quad (19)$$

From the above mathematical analysis, the different poses of the end effector result in

the change of the pose errors of outputs. In order to describe fully the standard deviations of $\delta \mathbf{E}_R$ and $\delta \mathbf{E}_S$, the estimation standard in the whole workspace between them should be established. Suppose that the volume of the workspace is V , it follows [22]:

$$\tau_{Ri} = \int_V \sqrt{\sum_{j=1}^6 T_{Rji}^2} dv. \quad (20)$$

The above equation can describe all error sources of the parallel manipulator in its workspace, however, it cannot achieve the further sensitivity analysis under the case of specific error compensation and identification. Therefore, a novel statistical model of sensitivity coefficients, to implement the unified process on the above error sources in the workspace is presented as:

$$\bar{\tau}_{Ri} = \frac{\tau_{Ri}}{\sum_{i=1}^{23} \tau_{Ri}}. \quad (21)$$

2 STRUCTURE CALIBRATION

2.1 Calibration Model of Kinematic Parameters

The mechanical structure of the parallel manipulator is assembled and the kinematic parameters can be identified by the calibration of kinematic parameters. In order to achieve the static mathematical compensation of the manipulator, it is necessary to modify the control model of kinematics according to the identified error parameters.

The pose of the end effector consists of three position parameters and three orientation parameters. In order to solve 23 kinematic parameters in $\delta \mathbf{E}_R$, it is necessary to measure four groups of the pose by the testing instruments of the end effector in every calibration. According to the kinematic model and its differential form of the parallel manipulator, Eq. (22) can be obtained:

$$\Delta \mathbf{E}_S = [\Delta \mathbf{E}_{S1}^T \ \Delta \mathbf{E}_{S2}^T \ \Delta \mathbf{E}_{S3}^T \ \Delta \mathbf{E}_{S4}^T]^T = \mathbf{J}_R \Delta \mathbf{E}_R, \quad (22)$$

where $\Delta \mathbf{E}_{Si} = [\Delta x_E, \Delta y_E, \Delta z_E, \Delta q_1, \Delta q_2, \Delta q_3]^T$, $i = 1, 2, 3, 4$. A group of the pose error of the end effector is represented as $\Delta \mathbf{E}_{Si}$. \mathbf{J}_R , a matrix of 24 rows and 23 columns, denotes the Jacobi matrix of calibration. The Eq. (22) can be changed as:

$$\Delta \mathbf{E}_R = \left[(\mathbf{J}_R^T \mathbf{J}_R)^{-1} \mathbf{J}_R^T \right] \Delta \mathbf{E}_S. \quad (23)$$

Implementing the Eq. (23) gives the iterative value compensating the matrix \mathbf{E}_R in the course of the kinematic calibration. The kinematic parameters can be calibrated by modifying the iterative value till the errors are less than the terminating value defined in advance. From Eq. (23), the matrix of the pose errors and the Jacobi matrix of calibration is needed to solve the iterative value. The corresponding procedures to obtain the matrices are shown as follows.

2.2 Analysis of the Pose Errors Matrix

Four groups of the pose of the end effector can be synthesized as the same expression. In order to describe the pose of the end effector, formulating the orientation matrix gives:

$$\mathbf{E}_W = \begin{bmatrix} \mathbf{D}_E & \mathbf{E}_{xyz} \\ 0 & 1 \end{bmatrix}, \quad (24)$$

where \mathbf{D}_E and \mathbf{E}_{xyz} denote the orientation matrix of the calibrated point and the geometrical vector of the calibrated point, respectively.

By calculating the orientation matrices based on the measured values and the theoretical values, the matrix of the pose errors is derived as the following equation:

$$\Delta \mathbf{E}_W = \mathbf{E}_W^{-1} (\mathbf{E}_{WS} - \mathbf{E}_W) = \begin{bmatrix} \Delta \mathbf{D}_E & \Delta \mathbf{E}_{xyz} \\ 0 & 1 \end{bmatrix}, \quad (25)$$

where \mathbf{E}_W and \mathbf{E}_{WS} denote the theoretical values solved by the kinematic model and the measured values, respectively. Herein, $\Delta \mathbf{E}_{xyz}$ equals to $[\Delta x_E \ \Delta y_E \ \Delta z_E]^T$.

The error of the orientation matrix $\Delta \mathbf{D}_E$ can be expressed as:

$$\Delta \mathbf{D}_E = \begin{bmatrix} 0 & \Delta D_{E12} & \Delta D_{E13} \\ \Delta D_{E21} & 0 & \Delta D_{E23} \\ \Delta D_{E31} & \Delta D_{E32} & 0 \end{bmatrix}, \quad (26)$$

where the expressions of elements in the matrix are the same as the above orientation matrix in the error model.

According to the relations between the elements of the error of the orientation matrix and the Quaternions parameters, the errors of the corresponding Quaternions parameters can be

obtained. The solutions of the matrix $\Delta \mathbf{E}_{S_i}$ can be achieved by substituting the errors of the pose and the Quaternions parameters into Eq. (22).

2.3 Analysis of Calibration Jacobi Matrix

Similar to the analysis of the pose errors, the Jacobi matrix of calibration consists of four submatrices denoted as \mathbf{J}_{R_i} . Because of the same expressions of the submatrices, the analysis of the Jacobi matrix of calibration can be simplified as the analysis of one submatrix, that is:

$$\mathbf{J}_{R_{ij}} = \frac{\partial \mathbf{E}_S}{\partial \mathbf{E}_{R_{ij}}}, j = 1, 2, \dots, 23. \quad (27)$$

According to the analysis of the error sensitivity, different error sources of kinematic parameters with the same error values have a different effect on the pose error of the end effector. It is essential to redefine the offset denoted as $\Delta e_{R_{ij}}$ in $\mathbf{J}_{R_{ij}}$ based on the sensitivity coefficients of the errors for calibrating better the end effector. And the offset can be written as:

$$\Delta e_{R_{ij}} = \frac{\Delta e_{E_{ij}}}{\tau_{R_i}}, \quad (28)$$

where $\Delta e_{E_{ij}}$ denotes the j^{th} offset that need to be calibrated.

By the derivation of the offsets, the Jacobi matrix of calibration can be derived as:

$$\mathbf{J}_{R_{ij}} = \begin{bmatrix} \frac{\Delta x_E}{\Delta e_{R_{ij}}} & \frac{\Delta y_E}{\Delta e_{R_{ij}}} & \frac{\Delta z_E}{\Delta e_{R_{ij}}} & \frac{\Delta q_1}{\Delta e_{R_{ij}}} & \frac{\Delta q_2}{\Delta e_{R_{ij}}} & \frac{\Delta q_3}{\Delta e_{R_{ij}}} \end{bmatrix}. \quad (29)$$

2.4 Calibration Algorithm of Kinematic Parameters

Measuring the practical lengths of the drive limbs and the corresponding pose of the end effector and calculating the theoretical values of the end effector, the kinematic parameters of every joint can be calibrated based on the successive approximation algorithm. The procedures of the calibration algorithm of the manipulator are shown in Fig. 2.

3 NUMERICAL SIMULATION

3.1 Sensitivity Simulation

Six groups of theoretical values and error values of the parallel manipulator are defined in Table 1.

Substituting the theoretical values into the kinematic model, the corresponding position-orientations of the end effector are obtained and shown in Table 2.

According to the statistical model of sensitivity coefficients, the pose errors of the end effector caused by the errors of kinematic parameters in the whole workspace can be calculated respectively. Normalizing the results of the above process gives the sensitivity percentages of twenty-three kinematic parameter errors in Eq. (13) shown as Fig. 3.

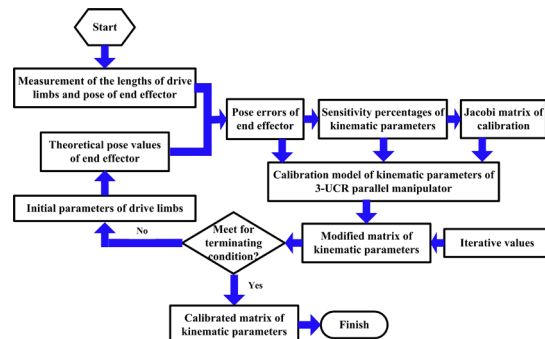


Fig. 2. Calibration algorithm of the kinematic parameters of the parallel manipulator

From Fig. 3 it is known that the kinematic parameters with symmetrical connectors, such as A_2 , a_2 , A_3 and a_3 , have a similar effect on the pose errors of the end effector and the result validates the sensitivity model by the structure characteristics. Comparatively, greater sensitivity percentages of the drive limbs represent that the actuator errors have more effect on the pose errors of the end effector. Due to the errors of some kinematic parameters, having the greater sensitivity percentages, it is essential to control the length errors between the origin in the absolute coordinate system and the joint connectors on the base, especially the errors along Z-axis perpendicular to the base. However, the length errors between the origin in the relative coordinate

system and the joint connectors on the moving platform and the errors of the end effector have less sensitivity percentages. Therefore, with the promise to guarantee the whole precision of the manipulator, it is feasible to adjust the manufacture and assembly tolerance of mechanical parts by the sensitivity percentages.

The symbol η denotes the structure scales which is the ratio of the fix radiuses of the base

and the moving platform. The variation of the sensitivity percentage of the kinematic parameters with different structure scales are given in Fig. 4.

Fig. 4 shows that, with the variation of the structure scale, the sensitivity percentages of kinematic parameters have not been changed obviously in corresponding reachable workspaces. On the other hand, it is necessary to strictly control the kinematic parameters with different structure

Table 1. Theoretical values and error values of the parallel manipulator

Title	Theoretical value [mm]	Error value [mm]	Title	Theoretical value [mm]	Error value [mm]
r_1	Six groups in the following table	0.02	$L_{O'a_x}$	$a_1 : 0; a_2 : 25\sqrt{3}; a_3 : -25\sqrt{3}$	0.05
r_2	Six groups in the following table	0.02	$L_{O'a_y}$	$a_1 : 50; a_2 : -25; a_3 : -25$	0.05
r_3	Six groups in the following table	0.02	$L_{O'a_z}$	$a_1 : z_{a_1}; a_2 : z_{a_2}; a_3 : z_{a_3}$	0.05
L_{OE}	220	0.08	L_{O_Ax}	$A_1 : 0; A_2 : 34\sqrt{3}; A_3 : -34\sqrt{3}$	0.05
L_B	$68\sqrt{3}$	0.08	L_{O_Ax}	$A_1 : 68; A_2 : -34; A_3 : -34$	0.05
L_m	$50\sqrt{3}$	0.08	L_{O_Ax}	$A_1 : 0; A_2 : 0; A_3 : 0$	0.05

Table 2. Theoretic values of limbs' lengths and output parameters

Group	r_1 [mm]	r_2 [mm]	r_3 [mm]	x_E [mm]	y_E [mm]	z_E [mm]	q_0	q_1	q_2	q_3
1	300.042	265.307	349.770	219.956	24	304.4	0.714	0	0.7	0
2	289.905	269.18	350.913	207.073	58.349	377	0.823	-0.15	0.55	0
3	287.356	273.15	350.147	195.375	72.150	392.4	0.843	-0.20	0.50	0
4	296.341	264.903	350.822	220.12	33.807	333	0.758	-0.05	0.65	0
5	346.459	308.792	263.091	-116.446	-169.831	395.7	0.847	0.40	-0.35	0
6	376.653	283.193	270.914	-28.924	-251.544	357.2	0.794	0.60	-0.10	0

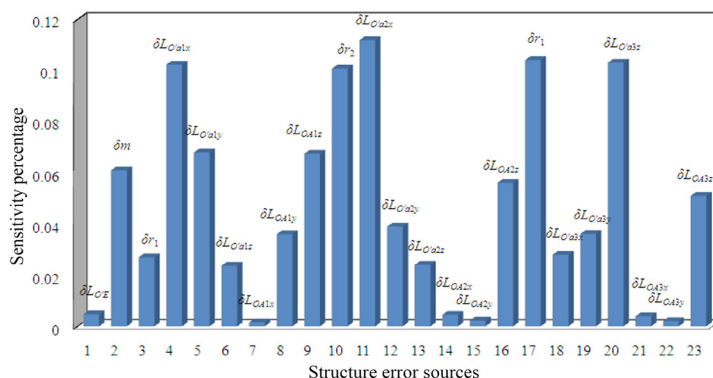


Fig. 3. Sensitivity percentages of kinematic parameters

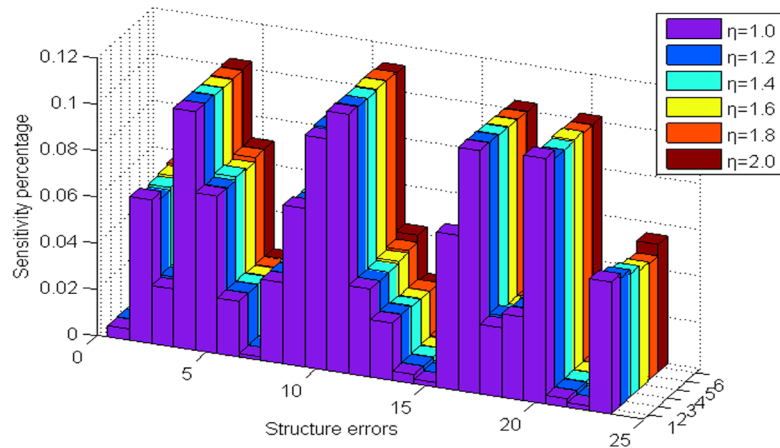


Fig. 4. Sensitivity percentage of kinematic parameters with different structure scales

Table 3. Poses of the end effector with four groups of limbs

Group	Length of drive limbs [mm]			Pose of the end effector [mm mm mm / / /]
	r_1	r_2	r_3	$[x_E, y_E, z_E, q_1, q_2, q_3]$
1	314.292	262.268	335.145	$[192.582, -49.6373, 369.397, 0.154879, 0.564173, 0]$
2	320.946	264.256	330.823	$[184.582, -77.5489, 323.506, 0.264831, 0.613548, 0]$
3	339.239	262.179	315.004	$[137.102, -146.751, 388.413, 0.359163, 0.412386, 0]$
4	349.929	263.507	306.072	$[107.704, -180.687, 394.056, 0.423459, 0.326984, 0]$

scales having greater sensitivity percentages.

3.2 Calibration Simulation

For validating the calibration algorithm of kinematic parameters, the iterative calculation of the given kinematic parameters by the numerical simulation is given as follows. The kinematic parameters are shown in Table 1, and the corresponding errors of these parameters are presented in $\Delta \mathbf{E}_R$:

$$\Delta \mathbf{E}_R = [-0.1, 0.1, 0.05, 0.08, -0.08, -0.08, 0.08, 0.08, -0.08, -0.05, 0.08, 0.08, -0.08, -0.08, 0.08, -0.08, 0.05, -0.08, -0.08, 0.08, -0.08, 0.08, 0.08]_{1 \times 23}^T,$$

where the errors of kinematic parameters $\Delta \mathbf{E}_R$ correspond to Eq. (13).

Substituting four groups of the kinematic parameters into the kinematic model of the manipulator, the corresponding poses of the end effector are shown in Table 3.

Taking the lengths of the drive limbs, the poses of the end effector in Table 3 and the values of the kinematic parameters in Table 1 into the kinematic calibration program of the parallel manipulator and calculating iteratively 7 times, the modified matrix of kinematic parameters is obtained. $\Delta \mathbf{E}_S$ denotes the corresponding norm of the pose errors of the end effector, it is less than the terminating value, defined as 0.01, which has no unit because of having no uniform unit in $\Delta \mathbf{E}_S$. After modifying 7 times, the values of the kinematic parameters converge gradually to the truth values which are the sums of the theoretical values and the given errors of the kinematic parameters in the numerical simulation.

The terminating time in the calibration program is decided by the absolute difference of the truth values and the modified kinematic parameters. For the purpose of representing the change of kinematic parameters, the changes of uncalibrated kinematic parameters and calibrated kinematic parameters are shown in Fig. 5.

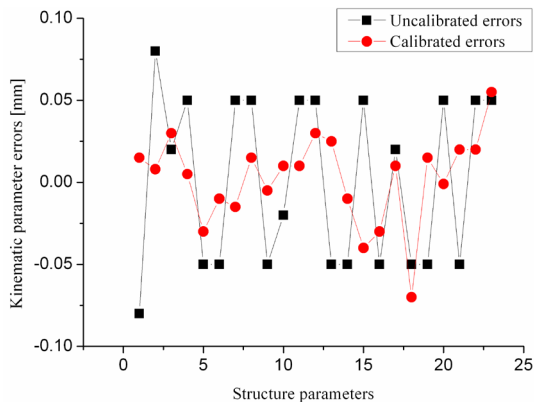


Fig. 5. Comparison of the uncalibrated kinematic parameters and calibrated kinematic parameters

Fig. 5 shows that most errors of calibrated kinematic parameters are decreasing greatly, especially the kinematic parameters with high sensitivity percentage, and the successive approximation algorithm based on the statistical sensitivity coefficients is validated. Because of the lower-mobility parallel manipulator, the errors of kinematic parameters caused by uncontrolled degree-of-freedom cannot be compensated completely. Most errors of kinematic parameters are less than the terminating value. On the contrary, due to the equilibration effect of the least squares method, some errors of calibrated kinematic parameters, such as $\delta L_{O_2a_3x}$ and $\delta L_{O_4a_3z}$, are increasing. In the course of calibration of kinematic parameters, the sensitivity coefficients and calibrated kinematic parameters with increasing errors have always lower sensitivity percentages partly decide the iterative value. The significance of the sensitivity conversion is emphasized by effectively decreasing the errors of kinematic parameters with higher sensitivity percentages. From the comparison in Fig. 5, the calibration algorithm has relatively fast convergence and concrete directivity when optimizing iteratively and is effective to study the calibration questions.

4 CONCLUSIONS

In this study, by the complete differential-coefficient matrix theory, the error model of the parallel manipulator was established. Then, the statistical model of sensitivity was derived by normalizing all error sources in the reachable

workspace. According to the results of sensitivity simulation, the sensitivity percentages of the kinematic parameters varied slightly with the variation of the structure scales. The kinematic parameters with higher sensitivity percentages which should be controlled strictly were distinguished. In the course of manufacture and assembly, decreasing the length errors between the origin in the relative coordinate system and the joint connectors on the base is essential, especially the error decrease along Z-axis perpendicular to the base.

Based on the successive approximation algorithm, the calibration model with sensitivity conversion was established. According to the corresponding simulation, the algorithm is effective to study the calibration question by comparing the values of every kinematic error and has relatively fast convergence when optimizing iteratively. With the conversion according to analytical results of sensitivity coefficients, the operation steps have concrete directivity.

The approach of the calibration proposed in this article can be applied to structure calibration not only of less-DOF but also of six-DOF parallel manipulators. When it is applied to the six-DOF parallel manipulator, all source errors according to six limbs should be considered, and the dimensions of corresponding matrices such as $\Delta \mathbf{E}_R$, \mathbf{T}_R and \mathbf{T}_2 would change accordingly, but the main analysis steps are the same as the application to the less-DOF parallel manipulators.

5 ACKNOWLEDGEMENTS

This research is supported by the National Natural Science Foundation of China (Grant No. 50905180) and the youth foundation of China University of Mining and Technology (Grant No. OE090191).

6 REFERENCES

- [1] Hunt, K.H. (1978). *Kinematic geometry of mechanisms*. Clarendon Press, Oxford, New York,.
- [2] Ryu, D., Song, J.B., Cho, C., Kang Kim, S.M. (2010). Development of a six DOF haptic master for teleoperation of a mobile

- manipulator. *Mechatronics*, vol. 20, p. 181-191.
- [3] Ropponen, T., Arai, T. (1995). Accuracy analysis of a modified Stewart platform manipulator. *IEEE International Conference on Robotics and Automation*, vol. 1, p. 521-525.
- [4] Wang, J., Masory, O. (1993). On the accuracy of a Stewart platform-Part I: The effect of manufacturing tolerances. *IEEE International Conference on Robotics and Automation*, vol. 1, p. 114-120.
- [5] Huang, T., Li, Y., Tang, G., Li, S., Zhao, X. (2002). Error modeling, sensitivity analysis and assembly process of a class of 3-DOF parallel kinematic machines with parallelogram struts. *Science in China: Series E*, vol. 45, no. 5, p. 467-476.
- [6] Alici, G., Shirinzadeh, B. (2006). Optimum dynamic balancing of planar parallel manipulators based on sensitivity analysis. *Mechanism and Machine Theory*, vol. 41, p. 1520-1532.
- [7] Pott, A., Kecskeméthy, A., Hiller, M. (2007). A simplified force-based method for the linearization and sensitivity analysis of complex manipulation systems. *Mechanism and Machine Theory*, vol. 42, p. 1445-1461.
- [8] Binaud, N. (2010). Sensitivity comparison of planar parallel manipulators. *Mechanism and Machine Theory*, vol. 45, no. 11, p. 1477-1490.
- [9] Merlet, J.P. (2006). *Parallel Robots*. Springer, Dordrecht.
- [10] Cedilnik, M., Soković, M., Jurkovič, J. (2006). Calibration and Checking the Geometrical Accuracy of a CNC Machine-Tool. *Strojniški vestnik - Journal of Mechanical Engineering*, vol. 52, no. 11, p. 752-762.
- [11] Zhuang, H., Masory, O., Yan, J. (1995). Kinematic calibration of a Stewart platform using pose measurement obtained by a single theodolite. *IEEE International Conference on Intelligent Robots and Systems*, p. 329-334.
- [12] Daney, D. (2003). Kinematic calibration of the Gough platform. *Robotica*, vol. 21, no. 6, p. 677-690.
- [13] Papa, G., Torkar, D. (2009). Visual Control of an Industrial Robot Manipulator: Accuracy Estimation. *Strojniški vestnik - Journal of Mechanical Engineering*, vol. 55, no. 12, p. 781-787.
- [14] Khalil, W., Besnard, S. (1999). Self calibration of Stewart-Gough parallel robot without extra sensors. *IEEE Trans. on Robotics and Automation*, vol. 15, no. 6, p. 1116-1121.
- [15] Chiu, Y., Perng, M. (2004). Self-calibration of a general hexapod manipulator with enhanced precision in 5-DOF motions. *Mechanism and Machine Theory*, vol. 39, p. 1-23.
- [16] Jeong, J., Kim, S., Kwak, Y. (1999). Kinematics and workspace analysis of a parallel wire mechanism for measuring a robot pose. *Mechanism and Machine Theory*, vol. 34, p. 825-841.
- [17] Chiu, Y., J., Perng, M.H. (2003). Self-calibration of a general hexapod manipulator using cylinder constraints. *International Journal of Machine Tools & Manufacture*, vol. 43, p. 1051-1066.
- [18] Hart, J.C., Francis, G.K., Kauffman, L.H. (1994). Visualizing quaternion rotation. *ACM Transactions on Graphics*, vol. 13, no. 3, p. 256-276.
- [19] Senan, N.A.F., O'Reilly, O.M. (2009). On the use of quaternions and Euler-Rodrigues symmetric parameters with moments and moment potentials. *International Journal of Engineering Science*, vol. 47, no. 4, p. 599-609.
- [20] Arribas, M., Elipe, A., Palacios, M. (2006). Quaternion and the rotation of a rigid body. *Celestial Mechanics and Dynamical Astronomy*, vol. 96, no. 3-4, p. 239-251.
- [21] Cayley, A. (1843). On the motion of rotation of a solid body. *Cambridge Math*, vol. 3, p. 224-232.
- [22] Gang, C., Luo Y. (2009). Study on structure design and dynamic performance of the parallel bionic robot leg. China University of Mining and Technology Press, Xuzhou.